High magnetoresistance in ultra-thin two dimensional Cr-based MXenes

Jianhui Yang,[a,b] Shaozheng Zhang,[a] Anping Wang,[a] Ruining Wang,[c] Chuan-Kui Wang,[,d] Guang-Ping Zhang,*[,d] and Liang Chen*[,b]*

[a] Quzhou University, Quzhou 324000, P. R. China

[b] Ningbo Institute of Materials Technology and Engineering, Chinese Academy of Sciences, Ningbo, Zhejiang, 315201, P. R. China. Email: chenliang@nimte.ac.cn.

[c] Hebei Key Lab of Optic-Electronic Information and Materials, College of Physics Science and Technology, Hebei University, Baoding 071002, People's Republic of China

[d] Shandong Province Key Laboratory of Medical Physics and Image Processing Technology, School of Physics and Electronics, Shandong Normal University, Jinan 250358, China. Email: zhangguangping@sdnu.edu.cn, ckwang@sdnu.edu.cn.

Support information

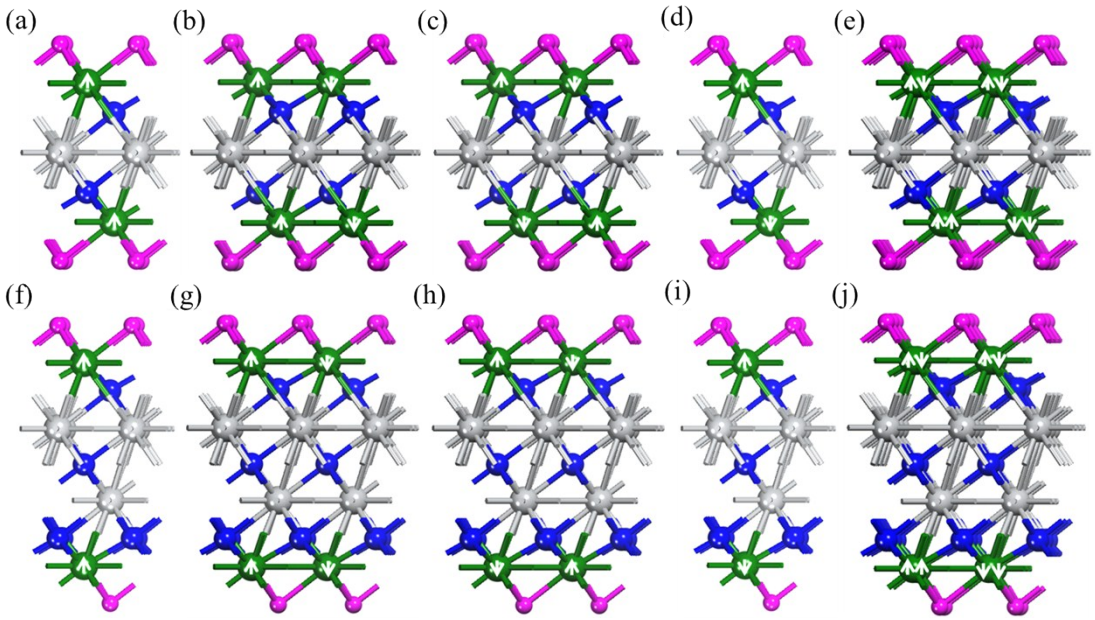

Fig. S1. (a)-(e) Side views of FM (a), AFM1 (b), AFM2 (c), AFM3 (d) and AFM4 (e) magnetic configurations for $Cr_2TiC_2F_2$. (f)-(j) Side views of FM (f), AFM1 (g), AFM2 (h), AFM3 (i) and AFM4 (j) magnetic configurations for $Cr_2Ti2C_3F_2$.

Table S1. Stable model and corresponding magnetic configuration, lattice constant (a), lattice mismatch (x), interlayer distances (d_1), thickness of MXene (d_2), E_{ad} between Au and MXene layers, magnetic moment for Cr atom (M_{Cr}) for Au-Cr_2CF_2-Au, Au-$Cr_2TiC_2F_2$-Au and Au-$Cr_2Ti_2C_3F_2$-Au sandwich structures.

Structures	*Lattice mismatch*	Adhesion Models	E_{ad} (eV/atom)	d_1(Å)	d_2(nm)	Magnetic state	M_{Cr} (μ_B)
Au-Cr_2CF_2-Au	3.3%	H_A	0.51	2.57	0.70	AFM3	±2.49
Au-$Cr_2TiC_2F_2$-Au	3.6%	H_A	0.53	2.56	0.96	AFM3	±2.59
Au-$Cr_2Ti_2C_3F_2$-Au	3.7%	H_A	0.56	2.52	1.21	FM	2.60

Table S2. Total energy (E) and magnetic moments of Cr atoms (Cr_{mag}) for Au-Cr_2CF_2-Au with Bridge (B), Hollow-A (H_A), Hollow-B (H_B) and Top (T) adsorption structures, respectively. The most stable magnetic states were bolded.

Adsorption Site	Magnetic State	E (eV/cell)	Cr_{mag} (μ_B)
B	NM	-71.156	0.000
	FM	-71.377	1.734
	AFM1	-71.274	±1.045
	AFM2	-71.378	±1.949
	AFM3	**-71.990**	**±2.492**
	AFM4	-	-
H_A	NM	-71.197	0.000
	FM	-71.417	1.730
	AFM1	-71.324	±1.041
	AFM2	-	-
	AFM3	**-72.032**	**±2.492**
	AFM4	-	-
H_B	NM	-71.179	0.000
	FM	-71.395	1.731
	AFM1	-71.300	±1.036
	AFM2	-	-
	AFM3	**-72.014**	**±2.490**
	AFM4	-	-
T	NM	-71.105	0.000
	FM	-71.358	1.716
	AFM1	-71.236	±1.048
	AFM2	-	-
	AFM3	**-71.902**	**±2.466**
	AFM4	-	-

Table S3. Total energy (E) and magnetic moments of Cr atoms (Cr_{mag}) for Au-$Cr_2TiC_2F_2$-Au with Bridge (B), Hollow-A (H_A), Hollow-B (H_B) and Top (T) adsorption structures, respectively. The most stable magnetic states were bolded.

Adsorption Site	Magnetic State	E (eV)	Cr_{mag} (μ_B)
B	NM	-90.039	±0.016
	FM	-91.151	2.595
	AFM1	-90.911	±2.384
	AFM2	-90.865	±2.346
	AFM3	**-91.218**	**±2.594**
	AFM4	-90.891	±2.385
H_A	NM	-90.056	0.000
	FM	-91.181	2.592
	AFM1	-90.946	±2.383
	AFM2	-90.899	±2.344
	AFM3	**-91.252**	**±2.591**
	AFM4	-90.925	±2.384
H_B	NM	-90.049	-0.001
	FM	-91.175	2.589
	AFM1	-90.941	±2.383
	AFM2	-90.894	±2.342
	AFM3	**-91.248**	**±2.591**
	AFM4	-90.940	±2.389
T	NM	-90.047	0.000
	FM	-91.124	2.615
	AFM1	-90.838	±2.358
	AFM2	-90.807	±2.329
	AFM3	**-91.147**	**±2.583**
	AFM4	-90.815	±2.344

Table S4. Total energy (E) and magnetic moments of Cr atoms (Cr_{mag}) for Au-$Cr_2Ti_2C_3F_2$-Au with Bridge (B), Hollow-A (H_A), Hollow-B (H_B) and Top (T) adsorption structures, respectively. The most stable magnetic states were bolded.

Adsorption Site	Magnetic State	E (eV)	Cr_{mag} (μ_B)
B	NM	-109.252	0.000
	FM	**-110.439**	**2.604**
	AFM1	-110.160	±2.352
	AFM2	-	-
	AFM3	-110.422	±2.624
	AFM4	-	-
H_A	NM	-109.286	0.000
	FM	**-110.469**	**2.602**
	AFM1	-110.174	±2.348
	AFM2	-	-
	AFM3	-110.454	±2.622
	AFM4	-	-
H_B	NM	-109.266	0.000
	FM	**-110.461**	**2.602**
	AFM1	-110.194	±2.353
	AFM2	-110.205	±2.370
	AFM3	-110.448	±2.622
	AFM4	-	-
T	NM	-109.268	0.000
	FM	**-110.423**	**2.616**
	AFM1	-110.080	±2.330
	AFM2	-110.081	±2.347
	AFM3	-110.379	±2.630
	AFM4	-	-

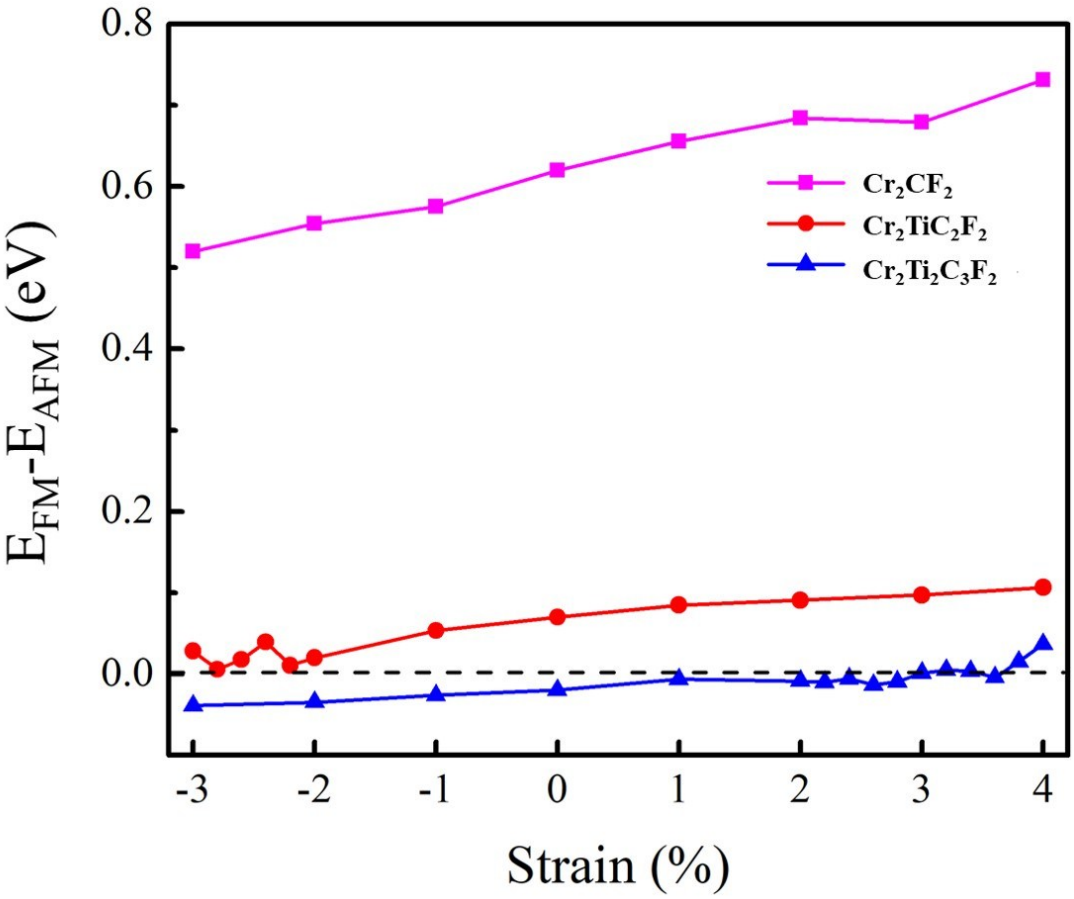

Fig. S2. ΔE (E_{FM}-E_{AFM}) of Au-Cr_2CF_2-Au, Au-$Cr_2TiC_2F_2$-Au, and Au-$Cr_2Ti_2C_3F_2$-Au with extensile strain.

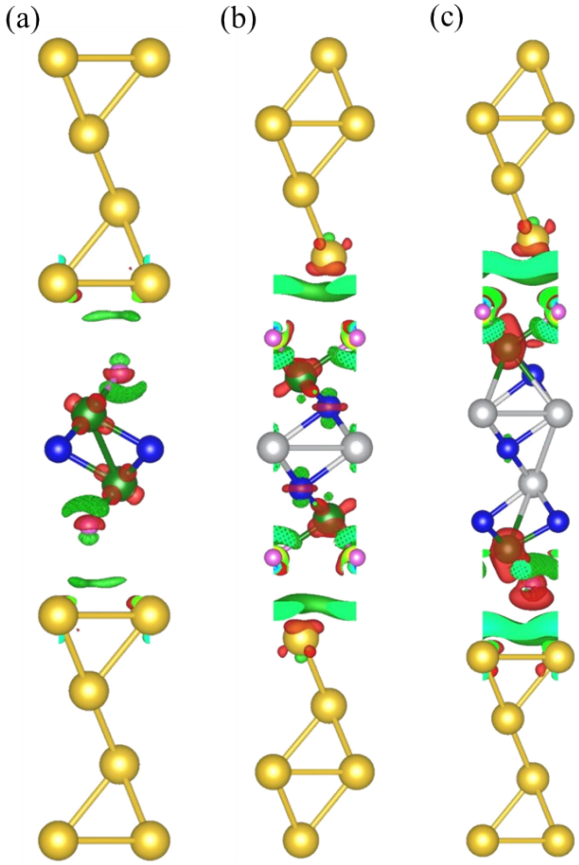

Fig. S3. Transfer charge for (a) Au-Cr_2CF_2-Au with AFM3 (b) Au-$Cr_2TiC_2F_2$-Au with AFM3 and (c) Au-$Cr_2Ti_2C_3F_2$-Au with FM magnetic structure, respectively. Isosurface value for (a), (b) and (c) was set to 0.0007 e/Å^3. Red and blue isosurface mean positive and negative region, respectively.

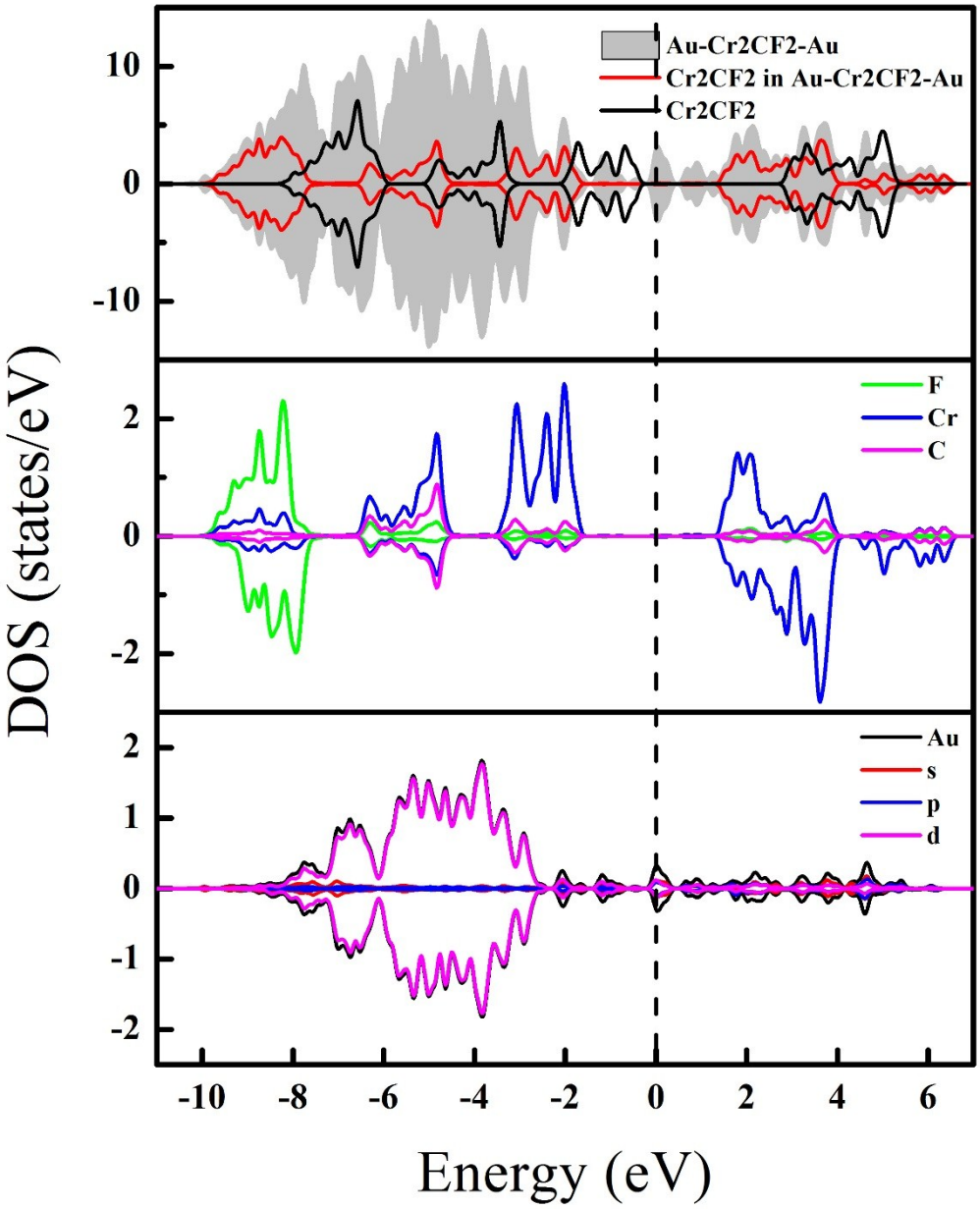

Fig. S4. PDOS of Au-Cr_2CF_2-Au in AFM configuration.

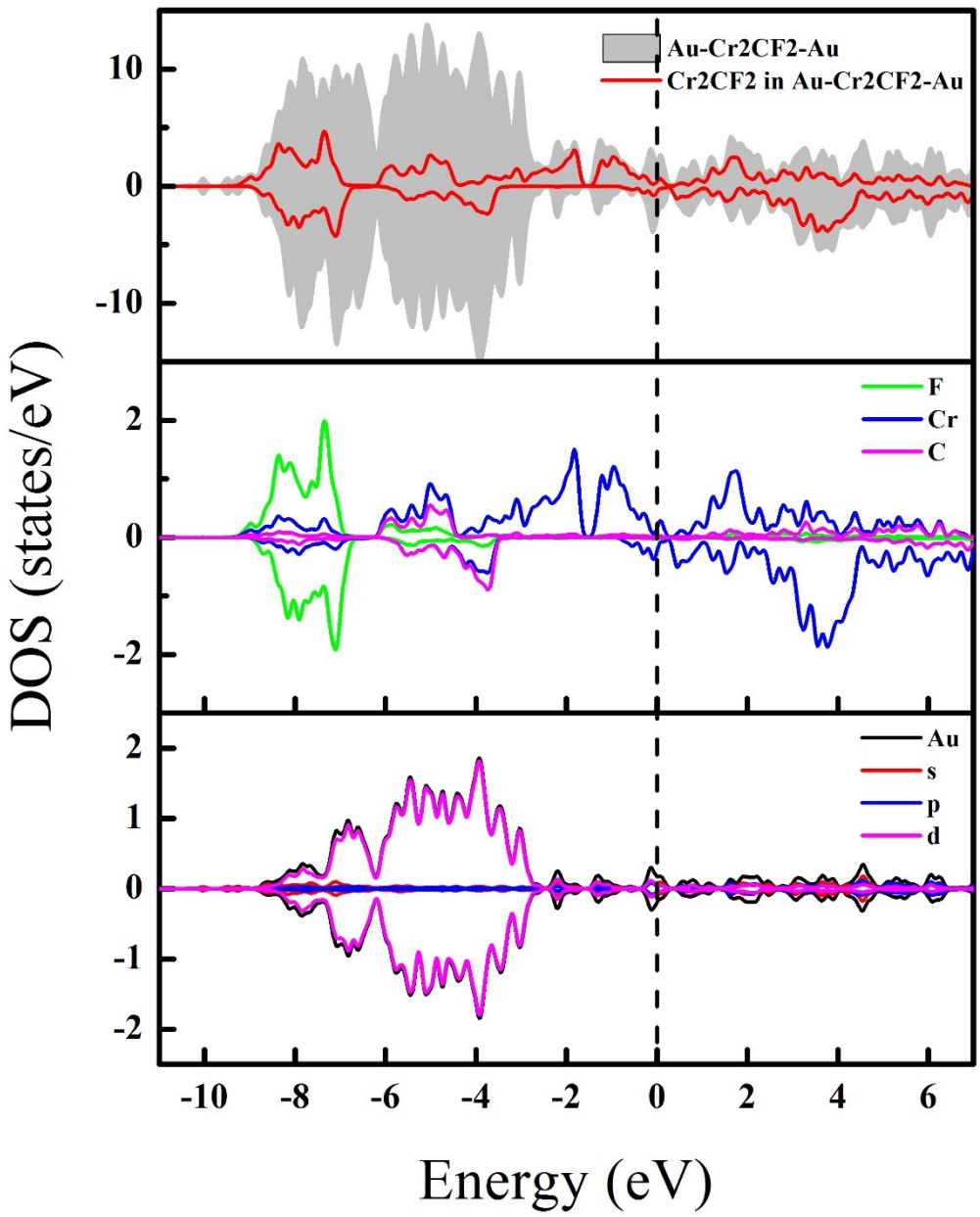

Fig. S5. PDOS of Au-Cr_2CF_2-Au in FM configuration.

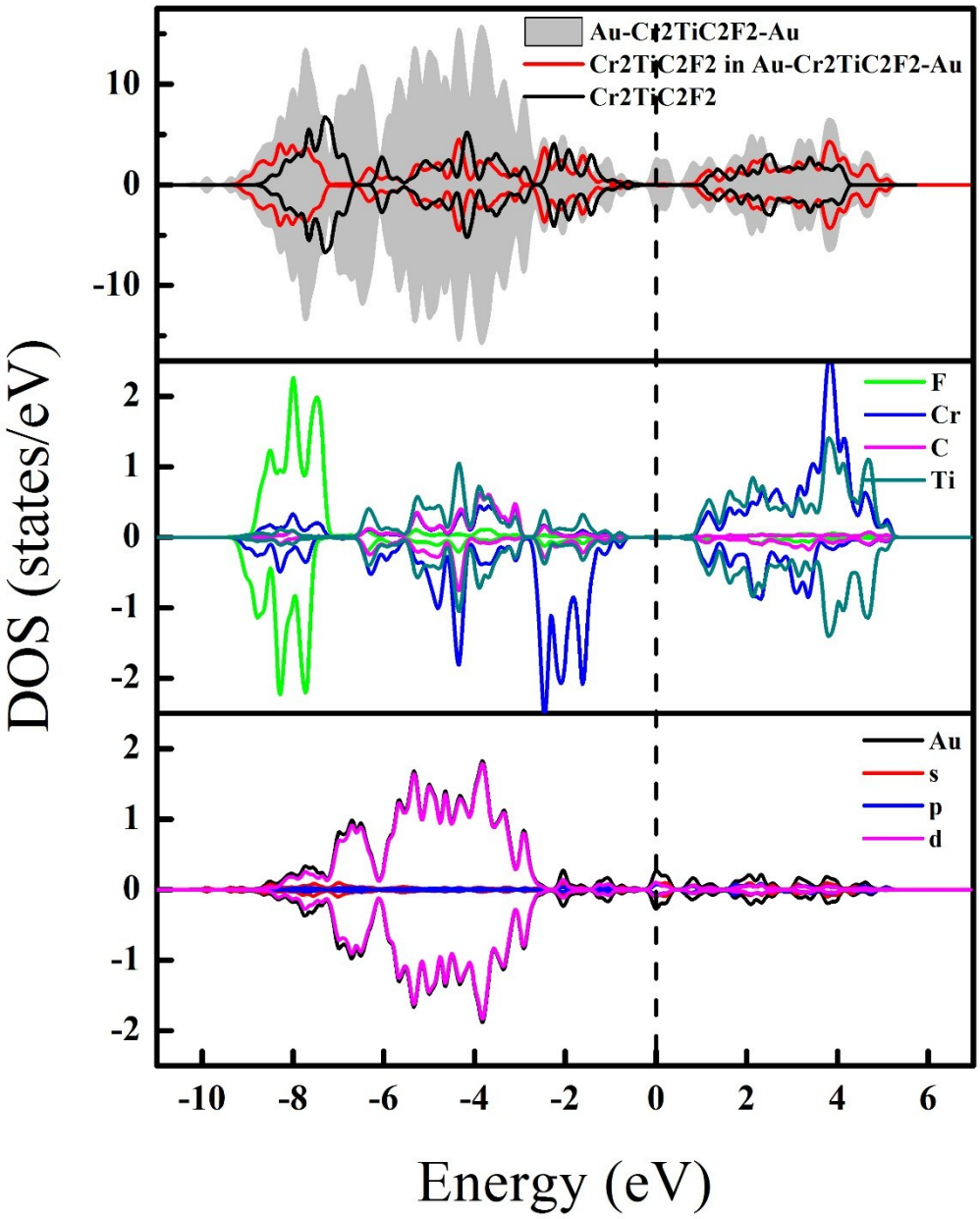

Fig. S6. PDOS of Au-$Cr_2TiC_2F_2$-Au in AFM configuration.

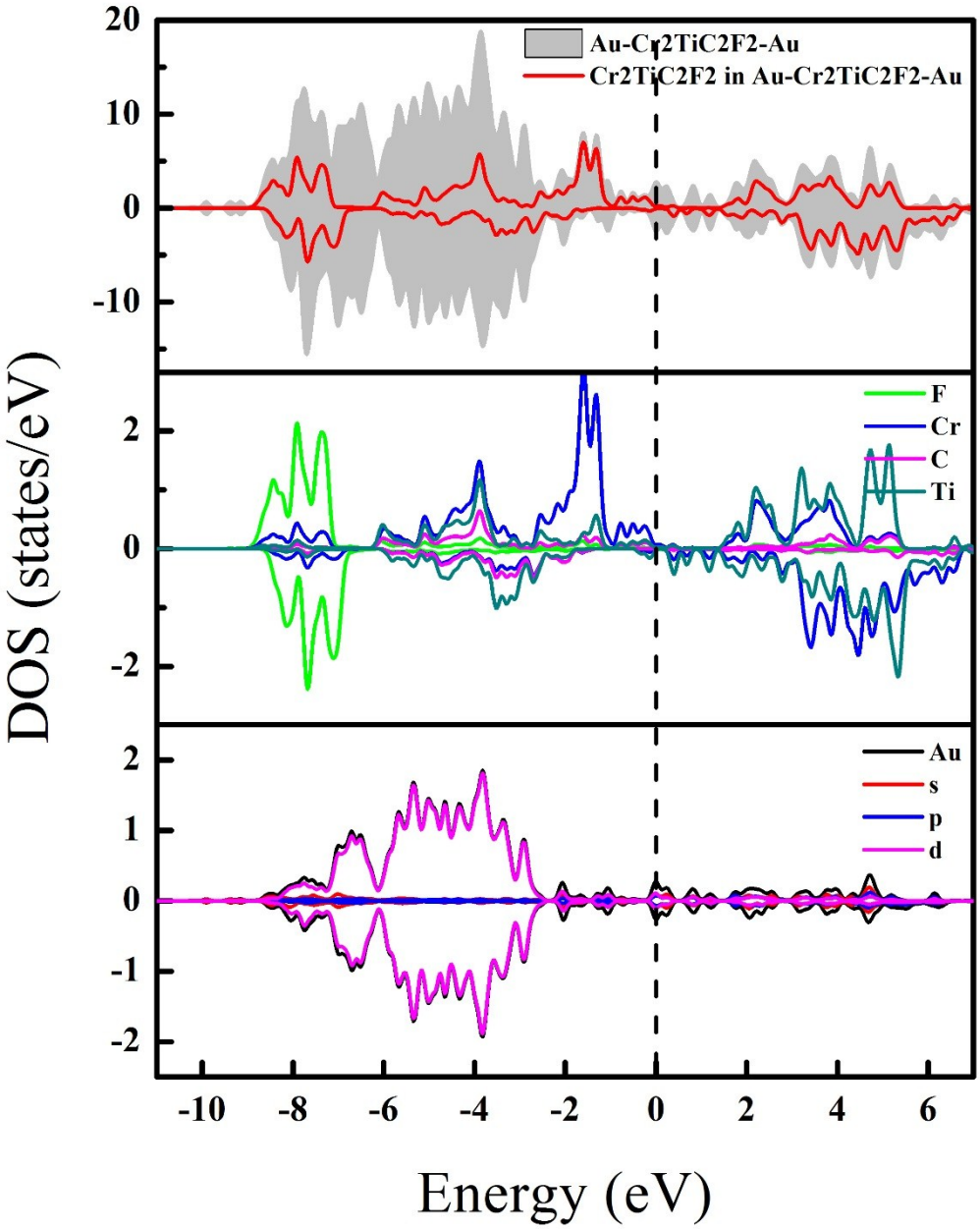

Fig. S7. PDOS of Au-$Cr_2TiC_2F_2$-Au in FM configuration.

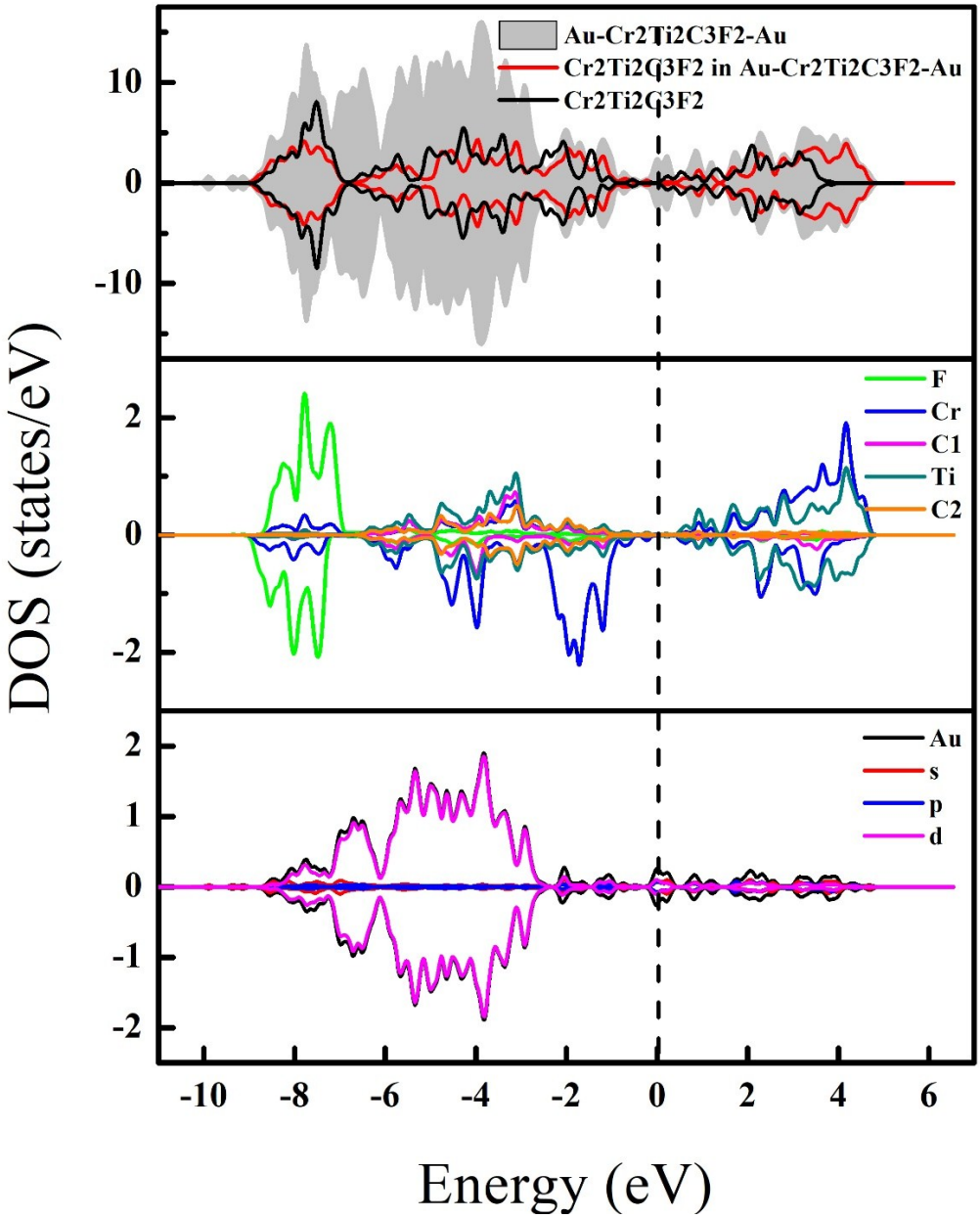

Fig. S8. PDOS of Au-$Cr_2Ti_2C_3F_2$-Au in AFM configuration.

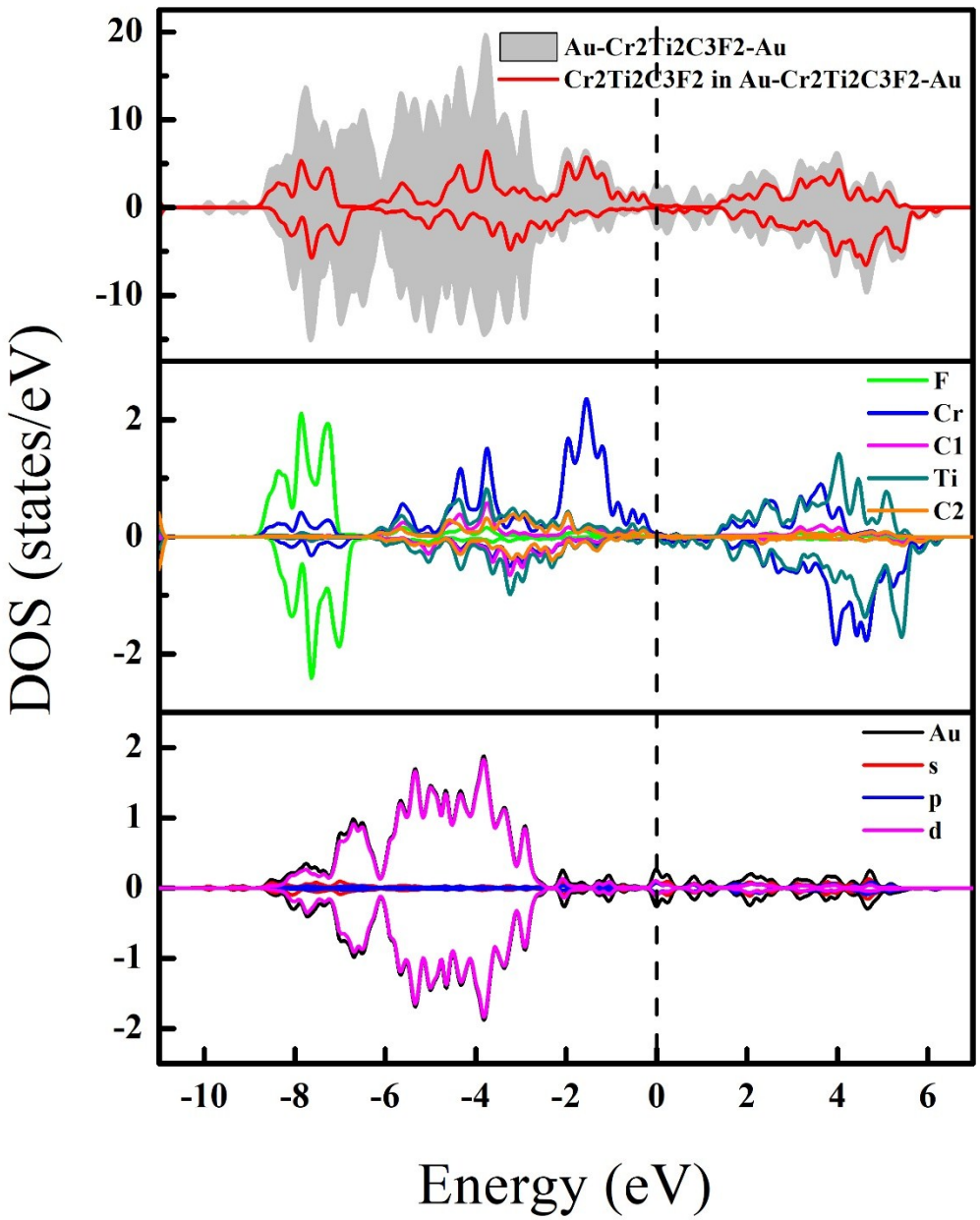

Fig. S9. PDOS of Au- $Cr_2Ti_2C_3F_2$-Au in FM configuration.